Extensive Ligand Rearrangements around the [2Fe-2S] Cluster of *Clostridium pasteurianum* Ferredoxin†

Marie-Pierre Golinelli,‡ Claire Chatelet,‡ Evert C. Duin,§ Michael K. Johnson,§ and Jacques Meyer*,‡

Département de Biologie Moléculaire et Structurale, CEA-Grenoble 38054 Grenoble, France, and Department of Chemistry and Center for Metalloenzyme Studies, University of Georgia, Athens, Georgia 30602

Received March 19, 1998; Revised Manuscript Received May 18, 1998

ABSTRACT: The [2Fe-2S] cluster of the ferredoxin from *Clostridium pasteurianum* is coordinated by cysteines 11, 56, and 60 and by a fourth cysteine, residue 24 in the wild-type protein, located on a flexible and deletable loop around residues 14−30. New mutated forms of this ferredoxin show that the fourth cysteine ligand can be located in any one of positions 14, 16, 21, 24, or 26. Another set of molecular variants has unveiled a new case of ligand swapping on the cysteine 60 ligand site. Replacement of cysteine 60 by alanine and introduction of a cysteine in position 21 yielded a ferredoxin that assembles a [2Fe-2S] cluster of which the ligands are cysteines 11, 21, 24, and 56. This cysteine ligand pattern is similar to that occurring in plant-type or mammalian-type ferredoxins, although the overall sequence similarities are below detection. Moreover, the vibrational and electronic properties of the resulting [2Fe-2S]$^{2+/+}$ center, as revealed by resonance Raman and EPR studies, are strikingly similar to those of mammalian-type ferredoxins. The extensive set of mutated forms of the *C. pasteurianum* ferredoxin now available indicates that cysteine ligand exchange may occur on residues 24 and 60, but not on residues 11 and 56. It is thus suggested that cysteines 24 and 60 are part of a solvent accessible aspect of the Fe−S cluster, whereas cysteines 11 and 56 are buried and form the more rigid part of the polypeptide ligand framework. In view of the unprecedented versatility of this [2Fe-2S] cluster and of its polypeptidic environment, the introduction of ligands other than cysteine in various positions has been attempted. These experiments have remained unsuccessful, and even including previous studies, noncysteinyl ligation has been obtained with this protein in only very few cases. The data provide an extensive confirmation that Fe−S clusters have a strong preference for thiolate ligation and rationalize the relatively rare occurrence of noncysteinyl ligation in native Fe−S proteins.

The [2Fe-2S] ferredoxin from the nitrogen-fixing saccharolytic anaerobe *Clostridium pasteurianum* (*Cp* 2Fe Fd)[1] is endowed with a number of unique properties which have been disclosed over the past years by biochemical and spectroscopic techniques and by site-directed mutagenesis (*1*−*8*). Of particular relevance here is the observation, made while identifying the cysteine ligands (residues 11, 24, 56, and 60) of the Fe−S cluster, that one of these ligands (cysteine 24 in the wild-type protein) could be displaced along a ten-residue segment, most likely belonging to a flexible loop, of the polypeptide chain (*7*). The mobility of this structural element was further assessed by the demonstration that deletions of variable length (3−14 residues) did not significantly alter the stability of the protein (*7*). These experiments confirmed the selective affinity of iron−sulfur clusters for thiolate ligands (*9*, *10*) and established this chemistry as a driving force able to direct structural reorganizations in proteins. The relevance of this phenomenon to the increasingly recognized role of iron−sulfur proteins in the regulation of cellular processes has prompted further investigation of the unusual interactions between the polypeptide chain and the [2Fe-2S] cluster in the *Cp* 2Fe Fd.

The molecular variants described hereafter have been prepared and characterized with the aim of further investigating the mobility of the flexible loop encompassing cysteines 14 and 24 and of exploring the possible occurrence of cysteine ligand swapping at other sites. The latter was suggested by the recent discovery of a gene encoding a putative protein of which the sequence is similar to that of the *Cp* 2Fe Fd, but the cysteine pattern is similar to that of plant ferredoxins (*11*). The results reported here show that the cysteine ligand distribution in *Cp* 2Fe Fd can be extensively manipulated and unveil new relationships among the various types of [2Fe-2S] proteins.

MATERIALS AND METHODS

All common DNA manipulations were as described (*5*, *12*, *13*). Enzymes were purchased from Boehringer Man-

†This work was supported by a grant from the National Institutes of Health (GM51962 to M.K.J.).

* Address for correspondence: DBMS-Métalloprotéines, CEA-Grenoble, 38054 Grenoble, France. Fax: (33) 4 76 88 58 72. E-mail: jacques.meyer@cea.fr.

‡ CEA-Grenoble.

§ University of Georgia.

[1] Abbreviations: *Cp*, *Clostridium pasteurianum*; *Cp* 2Fe Fd, [2Fe-2S] ferredoxin from *C. pasteurianum*; EPR, electron paramagnetic resonance; Fd, ferredoxin; PCR, polymerase chain reaction; RR, resonance Raman; VTMCD, variable temperature magnetic circular dichroism; WT, wild type.

S0006-2960(98)00639-4 CCC: $15.00
Published on Web 06/26/1998

Table 1: Generation of Mutated Genes[a]

mutation[b]	starting plasmid	mutagenic oligonucleotide[c]	
C11A	wild type	5′ GTCTACAACTAGTAGCAACGAAGATGTG 3′	(cds)
S13A/C14A/C24A	C14A/C24A	5′ CATTAAGTCTAGCAGCAGTACAAACGAAG 3′	(cds)
C14A/Q21C/C24A	C14A/C24A	5′ GTAAGCAAAACCGCACTGCTTTCCATTAAG 3′	(cds)
C14A/S26C/C24A	C14A/C24A	5′ CAACGGAATTTTTGCAGTAAGCAAAAC 3′	(cds)
C14A/S29C/C24A	C14A/C24A	5′ CTACAATTTCAACGCAATTTTTGGAGTAAG 3′	(cds)
C14A/L16M/C24A	C14A/C24A	5′ TTGCTGCTTTCCATTCATTCTAGCACTAG 3′	(cds)
C14A/C24M	C14A	5′ GGAATTTTTGGAGTACATAAAACCTTGCTGC 3′	(cds)
C14A/L16H/C24A	C14A/C24A	5′ GCTGCTTTCCATTATGTCTAGCACTAG 3′	(cds)
C14A/Q21H/C24A	C14A/C24A	5′ GGAGTAAGCAAAACCGTGCTGCTTTCC 3′	(cds)
C14A/C24H	C14A	5′ GAATTTTTGGAGTAATGAAAACCTTGC 3′	(cds)
C56A	C56S	5′ TAATACAGGTGCCTTTGGTATATGCAGTC 3′	(ncs)
C14A/C56A	C14A	5′ TAATACAGGTGCCTTTGGTATATGCAGTC 3′	(ncs)
C14A/Q21C/C56A	C14A/C56A	5′ GTAACAAAAACCGCACTGCTTTCCATTAAG 3′	(cds)
C56H,D,N	wild type	5′ TAATACAGGTVACTTTGGTATATGCAGTC 3′	(ncs)
C60A	wild type	5′ GCTTTGGTATAGCCAGTCAAGGCCC 3′	(ncs)
C60A/S61A	C60A	5′ CTTTGGTATAGCCGCTCAAGGCCCTATAG 3′	(ncs)
C60H,D,N/S61A	C60A/S61A	5′ GCTTTGGTATAVACGCTCAAGGCC 3′	(ncs)
C14A/C60A/S61A	C60A/S61A	5′ CCATTAAGTCTAGCACTAGTACAAACGAAG 3′	(cds)
C14A/C60H,D,N/S61A	C14A/C60A/S61A	5′ GCTTTGGTATAVACGCTCAAGGCC 3′	(ncs)
C14A/Q21C/C60A[d]	C14A	[d]	
C14A/Q21C/C60A/S61A	C14A/C60A/S61A	5′ GTAACAAAAACCGCACTGCTTTCCATTAAG 3′	(cds)
C11A/C14A/Q21C//C60A/S61A	C14A/Q21C/C60A/S61A	5′ GCACTAGTAGCAACGAAGATG 3′	(cds)
C14A/Q21C/C24A//C60A/S61A	C14A/Q21C/C60A/S61A	5′ GGAATTTTTGGAGTAAGCAAAACCGCACTG 3′	(cds)

[a] Mutagenic oligonucleotides were complementary to the coding strand (cds) or to the noncoding strand (ncs). In degenerate positions the symbol V is for A,G,C. Mutagenesis was performed with two rounds of PCR as described (*4*, *5*, *7*). [b] Mutations are noted with the one letter code for amino acids: the first letter indicates the original residue, the following number is its position in the sequence, and the second letter is the substituting residue. [c] Mutated bases (differing from the wild-type sequence) are underlined. [d] Mutations Q21C and C60A were introduced simultaneously by running two separate first rounds of PCR, one with each of the Q21C and C60A oligonucleotides, and by using the products of these reactions as primers for the second round of PCR.

nheim. Oligonucleotides were synthesized by phosphoramidite chemistry on a 381A Applied Biosystems synthesizer.

Site-directed mutagenesis was performed by a modification (*14*) of a method (*15*) which uses two successive rounds of polymerase chain reaction (PCR) to create a mutation and amplify a DNA fragment surrounding it. The DNA on which mutations were introduced was the pTCP2F plasmid (*13*), where a sequence encoding the *Cp* 2Fe Fd was cloned between the *Nde*I (5′ end) and *Hin*dIII (3′ end) restriction sites of the pT7-7 expression vector (*16*). The oligonucleotides used as mutagenic primers are listed in Table 1. The mutated plasmids were prepared as described (ref *5*; see also Table 1) and used to transform *Escherichia coli* K38 (HfrC λ) cells harboring the pGP1-2 plasmid (*16*). The overproduction and purification of the mutated proteins were carried out as reported (*5*).

Redox titrations were performed in a glovebox maintaining an oxygen concentration below 1.5 ppm. The reaction mixture (2.3 mL) contained 20 mM Tris/HCl, pH 7.4, 150 mM NaCl, 0.06 mM ferredoxin, and the following mediators: indigo disulfonic acid, safranine T, and benzyl viologen, each at a concentration of 2.5 μM. The potential was measured between the platinum electrode and the Ag/AgCl reference electrode of a combined electrode. Ferredoxin was titrated in both the reductive and the oxidative directions, with stepwise additions of dithionite or ferricyanide, respectively. UV−vis absorption spectra in the 300−800 nm range were recorded at each step, and the absorbance at 420 nm, where the contribution of the mediators was negligible, was used for the calculations (*17*). The redox potentials were obtained by averaging the values yielded by the reductive and oxidative titrations, which in all cases differed from each other by less than 10 mV.

UV−vis absorption spectra were recorded on a Hewlett-Packard 8452 diode array spectrophotometer. Resonance Raman (RR) spectra were recorded by collecting 90° scattering from the surface of a 10 μL frozen droplet of sample (20 K) on the coldfinger of an Air Products Displex DE-202 closed cycle helium refrigerator, using lines from Coherent Innova 10-W Ar^+ or 200-K2 Kr^+ lasers. The scattered light was analyzed using a ISA U-1000 double monochromator fitted with a cooled RCA 31034 photomultiplier tube with photon counting electronics. Circular dichroism (CD) spectra were recorded using a Jasco J-715 spectropolarimeter. This spectrometer was interfaced to an Oxford Spectromag 4000 superconducting magnet for variable-temperature magnetic circular dichroism (VTMCD) studies. The 50% (v/v) glycerol that was added to the VTMCD samples to ensure the formation of an optical glass on freezing had no effect on the EPR or UV−vis absorption spectra of the samples. X-band EPR spectra were recorded on a Bruker Instruments ESP 300D spectrometer equipped with an Oxford Instruments ESR 900 flow cryostat (4.2−300 K). The samples used for EPR and VTMCD studies were reduced anaerobically by sodium dithionite (2 mM final concentration) in a glovebox (<1 ppm O_2). Unless otherwise indicated, the samples for spectroscopic measurements were in 50 mM Tris/HCl buffer, pH 7.8.

RESULTS AND DISCUSSION

Mobility of the Fourth Cysteine Ligand on the Flexible Loop. Previous investigations had shown that one of the ligand sites of the [2Fe-2S] cluster of *Cp* 2Fe Fd could be occupied either by cysteine 24 (wild-type protein), by cysteine 14 (C24A variant), or by a newly introduced cysteine in position 16 (C14A/L16C/C24A variant) (*7*).

Table 2: Properties of Mutated *Cp* 2Fe Fd[a]

ferredoxin	purification yield[b]	A450/A280 ratio[c]	UV−vis absorption bands (nm)				redox potential[d]	EPR *g* values		
								g_1	g_2	g_3
wild type	1−2	0.50	336	420	464	550	−280	2.01	1.95	1.92
C24A	1−2	0.47	332	420	456	544	−358	2.01	1.95	1.92
C14A/C24A	1−1.5	0.37	322		442	560	−360	2.00	1.96	1.92
C14A/L16C/C24A	1.5	0.49	332	422	460	544	−300	2.01	1.96	1.92
C14A/Q21C/C24A	1	0.45	332	422	458	548	−355	2.01	1.96	1.92
C14A/S26C/C24A	0.5	0.39	328	424	456	560	nd	nd		
C14A/C24A/S29C	<0.1	0.06	324		454	560	nd	nd		
C60A[e]	0.15	0.35	328	422	460	550[f]	nd	nd		
C60A/S61A[e]	0.2	0.35	328	422	460	550[f]	nd	nd		
C14A/C60A/S61A[e]	<0.1	0.2	330	430	460[f]	550[f]	nd	nd		
C14A/Q21C/C60A	0.35	0.42	330	422	464	550[f]	nd	nd		
C14A/Q21C/C60A/S61A	1.1	0.47	330	422	464	550[f]	−406	2.01	1.94	1.92[g]

[a] nd, not determined. The following variants (not shown in this table) had UV−vis absorption spectra identical to that of C14A/C24A Fd: S13A/C14A/C24A, C14A/L16M/C24A, C14A/L16H/C24A, C14A/Q21H/C24A, C14A/C24M, and C14A/C24H. Other molecular forms not included in the table did not yield holoprotein: C11A, C56A, C56H, C56D, C56N, C14A/Q21C/C56A, C60H,D,N/S61A, C14A/C60H,D,N/S61A, C11A/C14A/Q21C/C60A/S61A, and C14A/Q21C/C24A/C60A/S61A. [b] Purification yield in milligrams per liter of culture after the last step, ion-exchange HPLC (*5*). [c] After the last purification step. [d] Redox potentials in millivolts versus the standard hydrogen electrode (see Materials and Methods). [e] Two forms having slightly different UV−vis absorption spectra were separated on ion-exchange HPLC. The characteristics of the major only are given here. [f] Weak and broad shoulder. [g] A sharp isotropic resonance is also observed at $g = 5.16$ in the low field region of this spectrum (see text).

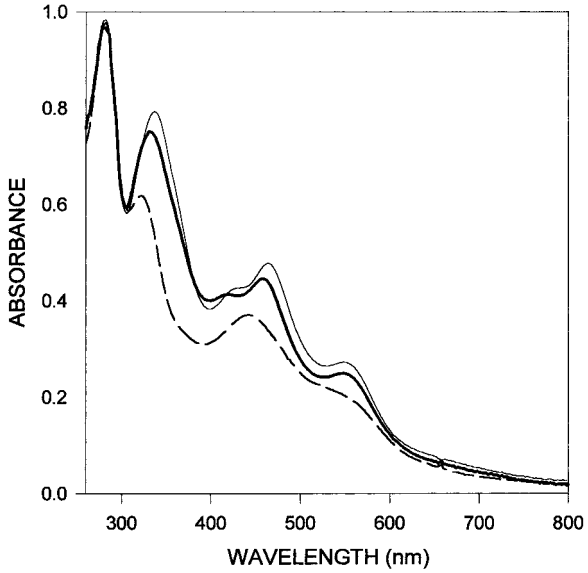

FIGURE 1: UV−vis absorption spectra of wild-type (thin solid line), C14/C24A (dashed line), and C14A/Q21C/C24A (thick solid line) *Cp* 2Fe Fd. The protein concentrations were 5 mg/mL, and the solvent was 0.5 M NaCl, 10 mM Tris/HCl buffer pH 8.0. The optical path length was 1 mm.

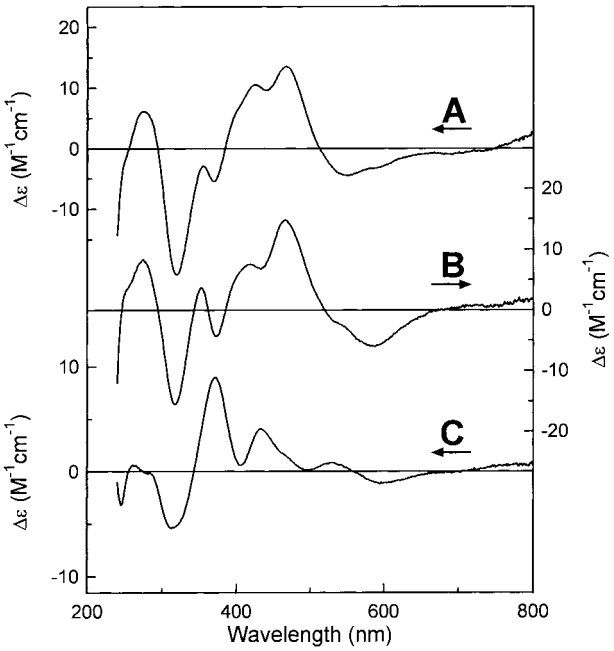

FIGURE 2: Room-temperature UV−vis CD spectra of oxidized Cp 2Fe Fd: (A) WT; (B) C14A/Q21C/C24A variant; and (C) C14A/Q21C/C60A/S61A variant. The solvent was 0.2 M NaCl, 50 mM Tris/HCl buffer pH 7.8, and the [2Fe-2S] chromophore concentrations were 0.60 mM (A), 0.32 mM (B), and 0.80 mM (C). The CD spectra are quantified with respect to the [2Fe-2S] chromophore concentrations.

These observations, together with deletions of variable length in this region of the sequence, pointed to the presence of a flexible loop encompassing these cysteine ligand positions. Information pertaining to the extent of this loop has been obtained by introducing cysteine residues in various other positions, taking as starting material the C14A/C24A variant that has only three cysteine residues; the C14A/Q21C/C24A, C14A/S26C/C24A, and C14A/C24A/S29C variants (Table 1) were thus prepared. With the newly introduced cysteine in position 21 or 26, recombinant holoproteins were obtained in yields reaching 50% of that of the WT protein (Table 2). The UV−vis absorption spectra of the C14A/Q21C/C24A (Figure 1) and C14A/S26C/C24A (not shown) variants display nearly identical positions of their absorption maxima (Table 2). They only differ by their A460/A280 ratio, which is higher in the case of the Q21C variant, an indication that the latter chromophore is more stable. As previously observed in the case of the C14A/L16C/C24A variant (*7*), the introduction of a cysteine in position 21 (Figure 1) or 26 (not shown) results in a reversion of the UV−vis spectral features of the C14A/C24A Fd toward those of the WT protein. The UV−vis CD spectra provide a much more sensitive monitor of the protein folding in the vicinity of the cluster than the absorption spectrum (Crouse et al., 1994). Hence, the close similarity in the CD spectra of the WT and the C14A/Q21C/C24A variant (Figure 2) attests to analogous protein folding patterns around the cluster. Since there are only three cysteine residues in the C14A/C24A variant, the

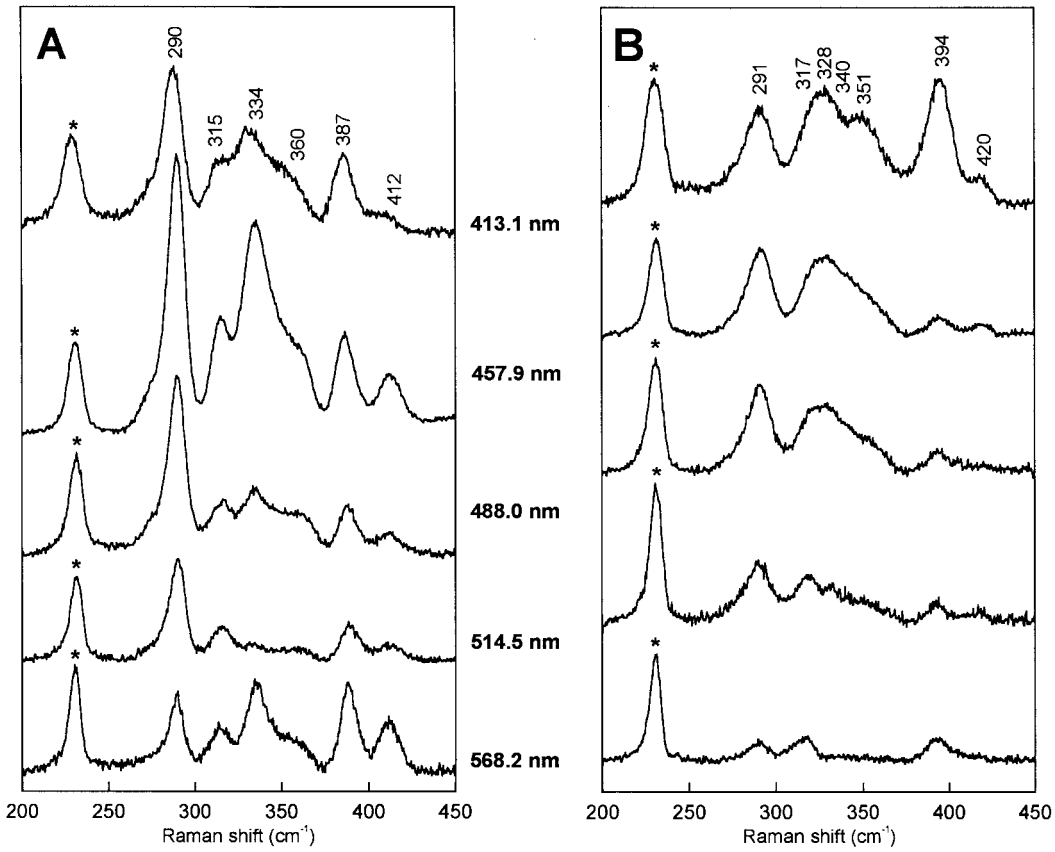

FIGURE 3: RR spectra of *Cp* 2Fe Fd: (A) C14A/Q21C/C24A variant; and (B) C14A/Q21C/C60A/S61A variant. The excitation wavelengths are indicated for each spectrum. The solvent was 0.5 M NaCl, 10 mM Tris/HCl buffer, pH 8.0, and the [2Fe-2S] chromophore concentrations were 2.5 mM (A) and 1.2 mM (B). Each spectrum is the sum of 20−30 scans with each scan involving photon counting for 1 s every 0.5 cm^{-1}, with 6 cm^{-1} spectral bandwidth. The sample temperature was 25 K. The peaks marked with an asterisk are due to frozen water, and the bands at 315 cm^{-1} (A) and 317 cm^{-1} (B) overlay weak bands arising from frozen water.

Table 3: Fe−S Stretching Frequencies and Provisional Assignments for WT and Mutated Forms of *Cp* 2Fe Fd and WT Adrenodoxin[a]

	Cp 2Fe Fd					adrenodoxin
mode[b]	WT	C24A	C14A/L16C/C24A	C14A/Q21C/C24A	C14A/Q21C/C60A/S61A	WT
$B_{2u}{}^{b}$	404	416	416	412	420	421
$A_g{}^{b}$	387	386	389	387	394	393
$B_{3u}{}^{b}$	366	360 (sh)[c]	360	360 (sh)	351	349
$B_{1u}{}^{t}$,$B_{2g}{}^{t}$	355	350	360	360 (sh)	340 (sh)	341
$A_g{}^{t}$	335	329	336	334	328	329
$B_{1g}{}^{b}$	313	310 (sh)	319 (sh)	315	317 (sh)	317
$B_{3u}{}^{t}$	290	284	288	290	291	291

[a] Assignments are based on the previous studies of WT *Cp* 2Fe Fd (*2*, *19*) and WT adrenodoxin (*18*). [b] Symmetry labels assuming an idealized D_{2h} point group for the $Fe_2S_2{}^{b}S_4{}^{t}$ core. [c] sh, shoulder.

logical interpretation of these results is that the cysteine incorporated in either position 21 or position 26 becomes the fourth ligand of the [2Fe-2S] cluster. The redox potential of the C14A/Q21C/C24A is −355 mV (Table 2), that is, 75 mV more negative than that of the WT Fd. Altogether, the full-length variants with the fourth cysteine in various positions on the flexible loop span the −280 to −358 mV redox potential range (ref *7*; Table 2).

Further support for the conclusion that the cysteine at position 21 in the C14A/Q21C/C24A variant assumes the role of the fourth cluster ligand comes from RR, EPR, and VTMCD studies. The RR spectra of the diamagnetic $[2Fe\text{-}2S]^{2+}$ center in the oxidized C14A/Q21C/C24A variant (Figure 3A) closely resemble those reported previously with the fourth cysteine at position 24 (WT), position 14 (C24A variant), and position 16 (C14A/L16C/C24A variant) (*7*), in terms of Fe−S stretching frequencies, relative intensities, and excitation profiles. Vibrational assignments and a comparison of the Fe−S stretching frequencies are given in Table 3. The minor differences in the Fe−S stretching frequencies that accompany changing the sequence location of the fourth cysteinyl ligand within the flexible loop region most likely reflect changes in the $Fe\text{-}S_\gamma\text{-}C_\beta\text{-}C_\alpha$ dihedral angle (*18*, *19*). EPR and VTMCD, taken together, provide an exquisitely sensitive probe of the ground- and excited-state electronic properties of the paramagnetic $[2Fe\text{-}2S]^{+}$ center in the reduced protein (*6*, *7*). The *g*-value anisotropy and g_{av} value of the reduced cluster are largely determined by the ligand field at the Fe(II) site of the localized valence $S = {}^1/_2$ $[2Fe\text{-}2S]^{+}$ cluster (*4*, *20*, *21*). Hence the near coincidence of the $S = {}^1/_2$ resonances, $g = 2.01$, 1.95−1.96, 1.92 (the spectrum for the C14A/Q21C/C24A variant is shown

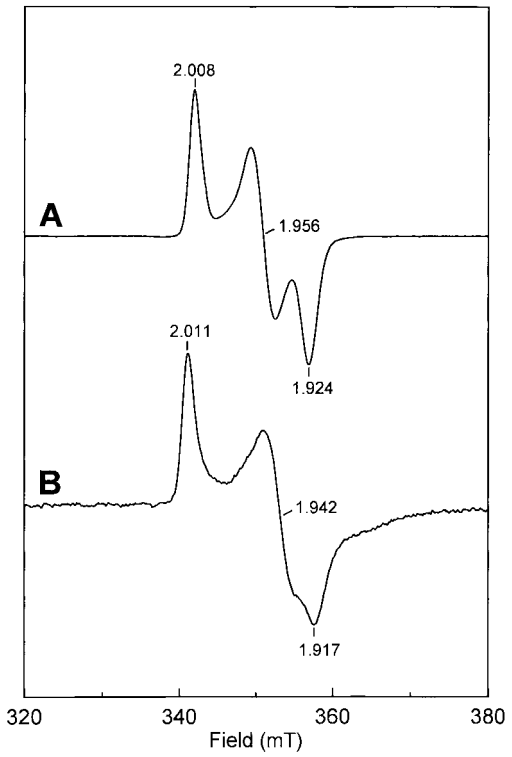

FIGURE 4: EPR spectra of dithionite-reduced *Cp* 2Fe Fd: (A) C14A/Q21C/C24A variant; and (B) C14A/Q21C/C60A/S61A variant. The [2Fe-2S] chromophore concentrations were 0.6 mM (A) and 0.9 mM (B), and the solvent was 0.5 M NaCl, 10 mM Tris/HCl buffer, pH 8.0, with 50% (v/v) glycerol. Conditions of measurement: (A) temperature, 20 K; microwave power, 2 mW; microwave frequency, 9.612 GHz; modulation amplitude, 0.64 mT. (B) temperature, 60 K; microwave power, 0.2 mW; microwave frequency, 9.597 GHz; modulation amplitude, 0.64 mT.

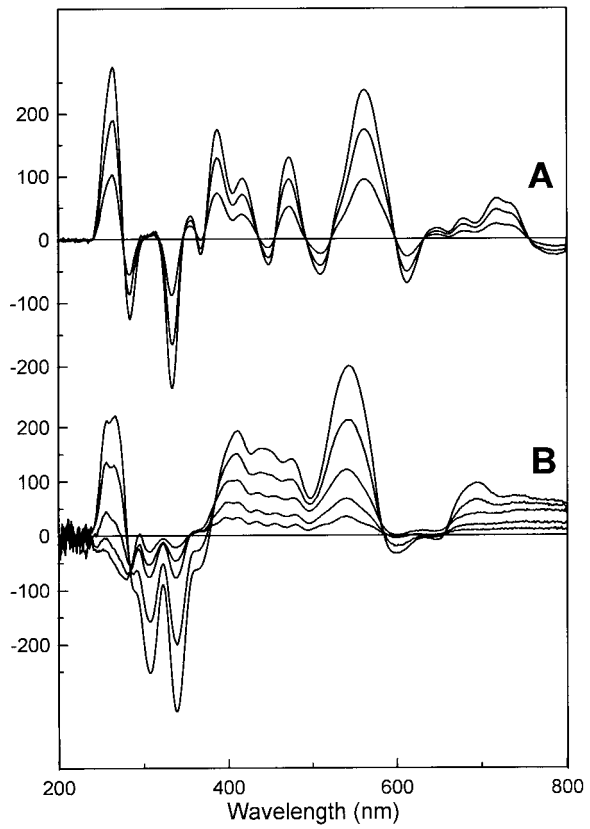

FIGURE 5: VTMCD spectra of dithionite-reduced *Cp* 2Fe Fd: (A) C14A/Q21C/C24A variant; and (B) C14A/Q21C/C60A/S61A variant. The spectra were recorded in 1 mm path length cuvettes with a magnetic field of 6.0 T at temperatures of 1.7, 4.2, and 10.0 K (A) and 1.6, 4.2, 10.6, 20.1, and 46.8 K (B). All bands increase in intensity with decreasing temperature. The samples were as described in Figure 4.

in Figure 4A), with the fourth cysteine at position 14, 16, 21, or 24, indicates that the ligand in the flexible loop coordinates the nonreducible Fe site and that changes in sequence location of this ligand do not alter the site of reduction. The correspondence in the ground-state properties extends to the excited-state structure as evidenced by the VTMCD spectra of the reduced proteins. VTMCD spectra for the reduced C14A/Q21C/C24A variant are shown in Figure 5A, and the one-to-one correspondence in positive and negative bands compared to the spectra reported for WT, C24A, and C14A/L16C/C24A (*7*) attests to identical primary coordination environments for the $[2Fe\text{-}2S]^{+}$ clusters. The close correspondence in the spectra in the S-to-Fe(III) charge-transfer region complements the EPR results by providing direct evidence for bis-cysteinyl ligation at the Fe(III) site (*19*).

When the cysteine was incorporated in position 29 (C14A/C24A/S29C), the protein assembled a very unstable chromophore (Table 2) having a UV−vis absorption spectrum very similar to that of the C14A/C24A variant, which indicated that cysteine 29 is unable to become a ligand of the cluster and that its introduction on the C14A/C24A background significantly destabilizes the protein. These molecular variants, together with those previously described (*7*), show that the mobility of the fourth cysteine ligand is restricted to the 14−26 segment of the polypeptide chain, which is still a considerable range. These observations are consistent with data showing that the stability of the protein was impaired by deletions extending beyond residue 30 (*7*) and with secondary structure predictions suggesting the initiation of an α-helix near residue 30.

Mutations Aimed at Obtaining Noncysteinyl Ligated Clusters. The presence of a flexible loop with high coordinating power in the vicinity of the [2Fe-2S] active site provided an opportunity for preparing new forms of noncysteinyl ligated Fe−S clusters. Thus, on the C14A/C24A variant having only three cysteines, several noncysteinyl residues having the potential of coordinating Fe−S clusters have been introduced in various positions (Table 1). However, neither the introduction of a methionine in position 16 or 24 nor the introduction of a histidine in position 16, 21, or 24 resulted in any modification of the UV−vis spectrum of the C14A/C24A variant. It should be recalled that the C14S/C24A and C14A/C24S variants were also found to be identical with C14A/C24A (*5*), an indication that a serine in position 14 or 24 cannot ligate the Fe−S cluster. Furthermore, the possible involvement of serine 13 in the ligation of the C14A/C24A chromophore has now been dismissed by showing that the S13A/C14A/C24A variant was also identical with the C14A/C24A one (Table 2). These results show that neither histidine, nor methionine, nor serine can become ligands of the [2Fe-2S] chromophore even though they belong to a flexible loop (residues 14−26) allowing cysteine residues in the same positions to become ligands. The high affinity of thiolate ligands for iron−sulfur clusters in synthetic models (*9*) as well as in proteins (*7*, *22*) is thus confirmed. Noncysteinyl ligation in proteins probably

requires a larger stabilizing contribution from the polypeptide chain than cysteinyl ligation.

Ligand Substitutions on Cysteines 11 and 56. As a relatively stable polypeptide framework is required for the stabilization of Fe−S clusters, the very unusual flexibility of the polypeptide chain of *Cp* 2Fe Fd near cysteines 14 and 24 was not expected to occur near any of the other ligand sites. Indeed, the significant destabilization of the C11S chromophore (*5*) suggested that no cysteine residue (cysteine 14 might have been a candidate) could easily substitute for the mutated cysteine 11 as a ligand of the chromophore. This inference has been substantiated by showing that no chromophore is assembled in the C11A variant (Table 2). The C56S variant has been found to assemble a stable serine-ligated chromophore (*4*, *5*) which has been investigated in detail (*5*, *6*, *8*, *23*). In contrast, the C56A mutated form is unable to do so, indicating that no other ligand can have access to this site. Furthermore, even when cysteine 56 was replaced by potentially coordinating residues, such as in the C56H, C56N, and C56D variants, no chromophore was detected (quoted in ref *24*). Thus, the polypeptide chain around cysteines 11 and 56 must be too constrained to allow access of incoming ligands to the corresponding coordination sites, or replacement of these cysteines by residues differing significantly from cysteine by their bulkiness or chemical properties.

Ligand Substitutions on Cysteine 60. As in the case of cysteine 56, the replacement of cysteine 60 by serine yielded a stable serine-ligated cluster (*4*−*6*, *8*, *23*). The behavior of the C60A variant, however, was not as clear-cut as that of the C56A one: whereas no chromophore is assembled in the C56A variant, expression of the C60A mutated gene in *E. coli* allowed the purification of small but significant amounts of *Cp* 2Fe Fd holoprotein having an acceptable (0.35) A450/A280 ratio (Table 2). This suggested that cysteine 60 could in some way, though rather inefficiently, be replaced by other ligands. The involvement of serine 61 was dismissed by showing that the UV−vis absorption of the C60A/S61A variant did not differ significantly from that of the C60A. In contrast, the possible involvement of cysteine14 as a substitute for cysteine 60 was suggested by the observation that its removal, in the C14A/C60A/S61A variant, further destabilizes the chromophore as compared to that of the C60A/S61A protein (Table 2), and in particular causes the coalescence of the 420−460 nm pair of absorption bands characterizing all-cysteine ligation in [2Fe-2S] clusters (*7*) into a broad band centered around 430 nm (Figure 6, Table 2). The latter feature has previously been observed in the C14A/C24A Fd (Figure 1; ref *5*), of which the polypeptide chain also contains only three cysteine residues. In both cases, the addition of excess thiolate (dithiothreitol or 2-mercaptoethanol) resulted in the development of features, in particular the two bands at about 420 and 460 nm, reminiscent of the WT spectrum (not shown). Thus, substitutes for cysteine 24 (*5*, *7*) or cysteine 60 are available, even in the absence of cysteine 14, when these ligands are replaced by alanine. The lability of the substituting ligands would be consistent with the involvement of water or hydroxide ion, as previously suggested for the C14A/C24A variant (*5*, *7*, *25*). Mutated forms of *Cp* 2Fe Fd having cysteine 60 replaced by histidine, aspartate, or asparagine have been prepared in both the C60A/S61A and C14A/C60A/S61A backgrounds (Table 1). The UV−vis absorption spectra of these variants in the 300−600 nm range were found not to differ from those of the C60A/S61A and C14A/C60A/S61A proteins, respectively (not shown), an indication that none of these newly introduced residues were able to coordinate the [2Fe-2S] cluster.

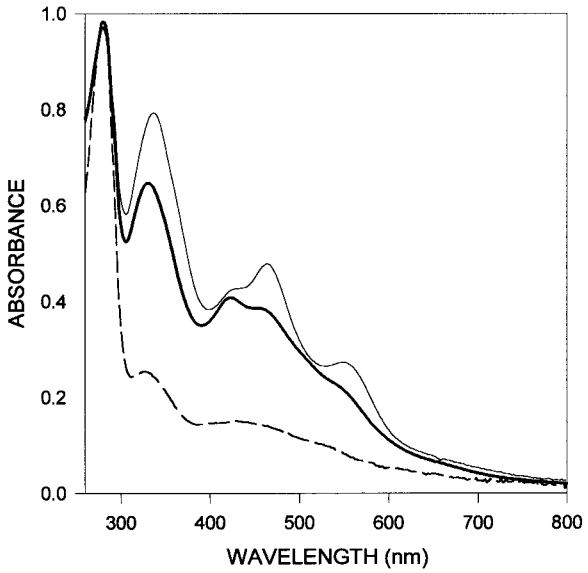

FIGURE 6: UV−vis absorption spectra of wild-type (thin solid line), C14/C60A/S61A (dashed line), and C14A/Q21C/C60A/S61A (thick solid line) *Cp* 2Fe Fd. The protein concentrations were 5 mg/mL, and the solvent was 0.5 M NaCl, 10 mM Tris/HCl buffer, pH 8.0. The optical path length was 1 mm.

Overturning the Cysteine Ligand Pattern in Cp 2Fe Fd. The assembly of chromophores, albeit relatively unstable ones, in the C60A set of variants (see above) suggests that the corresponding ligand site is relatively accessible and could therefore be filled, in the absence of cysteine 60, by another cysteine appropriately positioned in the polypeptide chain. A promising ligand position has been inferred from the sequence of a gene encoding a plant (*Solanum tuberosum*) enzyme with sucrolytic activity (*11*). The putative product of this gene is a 322-residue polypeptide comprised of several domains, of which one (residues 115−215) displays a high sequence similarity with *Cp* 2Fe Fd (*11*), suggesting that the two polypeptides are likely to assume similar folds. The distribution of the four cysteine residues occurring in this region of the putative plant sucrolytic enzyme does not quite match the cysteine ligand pattern of *Cp* 2Fe Fd: cysteines 123 and 135 of the former protein are the counterparts of cysteines 11 and 24 of *Cp* 2Fe Fd, and cysteine 161 of the plant enzyme is offset by only a few residues from cysteine 56 of *Cp* 2Fe Fd. A major discrepancy, however, is the absence, in the plant enzyme, of a cysteine residue corresponding to cysteine 60 of *Cp* 2Fe Fd, and the presence of a cysteine residue in a position matching glutamine 21 of *Cp* 2Fe Fd (Figure 7). This observation, despite the lack of evidence that the plant enzyme assembles a [2Fe-2S] cluster, suggested that a cysteine in position 21 of *Cp* 2Fe Fd might be able to replace the mutated cysteine 60. The Q21C mutation has therefore been introduced on both the C14A/C60A and C14A/C60A/S61A backgrounds. The resulting C14A/Q21C/C60A and C14A/Q21C/C60A/S61A variants both contain only four cysteines in positions 11, 21, 24, and 56, closely matching the distribution of cysteines in the plant

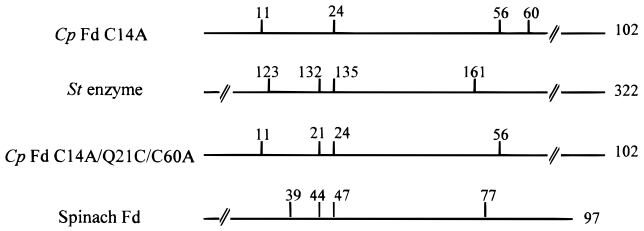

FIGURE 7: Scheme comparing cysteine ligand patterns in *Cp* 2Fe Fd, putative plant sucrolytic enzyme (*St* enzyme, from *Solanum tuberosum*, ref *11*), and spinach Fd (*34*). The ends of the sequences have been shortened when necessary (slashes). Mammalian-type Fds have not been included in this alignment because their cysteine ligand patterns are very similar to those of plant-type Fds.

enzyme (Figure 7) and resembling those established for plant-type and mammalian-type Fds, $C-X_4-C-X_2-C-X_{29}-C$ and $C-X_5-C-X_2-C-X_{36}-C$, respectively (*26*). Upon expression in *E. coli* of both mutated genes, recombinant holoproteins were obtained in yields showing that the introduction of a cysteine in position 21 stabilizes considerably the chromophore. The yield of the C14A/Q21C/C60A/S61A variant, at more than 50% of that of the WT, was about 3-fold higher than that of the C14A/Q21C/C60A variant (Table 2). For a yet unknown reason, the replacement of serine 61 by alanine stabilizes the chromophore. Since the UV−vis absorption spectra of the two variants appeared to be identical, only the quadruply mutated protein has been investigated in further detail.

Upon introduction of the Q21C mutation on the C14A/C60A/S61A background, the UV−vis absorption greatly increases in the 300−800 nm range (Figure 6), and the A450/A280 ratio nearly reaches the WT value (Table 2), which indicates an efficient stabilization of the chromophore by the polypeptide chain. Also, the partial reversion to wild-type-like features is a strong indication that the newly introduced cysteine 21 has become a ligand of the [2Fe-2S] cluster. However, whereas the UV−vis spectra of the C14A/L16C/C24A and C14A/Q21C/C24A variants are nearly superimposable on that of the WT protein (*7*), the spectrum of the C14A/Q21C/C60A/S61A Fd (Figure 6, Table 2) displays significant differences. These are mainly in the inversion of the relative intensities of the 422 and 464 nm bands and in the weakening of the 550 nm band. Such features are reminiscent of the spectra of plant-type and mammalian-type Fds. For example, the positions of the main bands, 330, 422, and 464 nm, of the C14A/Q21C/C60A/S61A Fd are within 2 nm of those of their counterparts in plant Fd (*27*). In contrast, the marked difference in the UV−vis CD spectra of the C14A/Q21C/C60A/S61A variant compared to those of WT (Figure 2) or of plant- and mammalian-type Fds (*28*, *29*), indicates dramatically different protein folding in the vicinity of the cluster as a result of a cluster-driven protein conformational change. Although the sensitivity of the UV−vis CD to the protein environment is useful for identifying major conformational changes in the vicinity of the cluster, the present data underscore the limited utility of CD as a means of identifying cluster type.

Spectroscopic investigations using RR and EPR reveal that the vibrational and electronic properties of the $[2Fe-2S]^{2+,+}$ center in the C14A/Q21C/C60A/S61A variant are very similar to those of mammalian-type Fds. RR spectra of the oxidized protein in the Fe−S stretching region are shown in Figure 3B. Although the bands are poorly resolved (possibly due to sample heterogeneity, see below), the vibrational frequencies and relative enhancement patterns of discrete bands are very similar to those of adrenodoxin, the archetypal mammalian Fd. The vibrational frequencies are compared with those of adrenodoxin in Table 3, and the strong enhancement of the totally symmetric A_g^b Fe−S stretching mode with violet (406 or 413 nm) excitation is a characteristic feature of mammalian-type 2Fe Fds (*18*). Likewise, the almost axial EPR spectrum of the reduced C14A/Q21C/C60A/S61A variant in the $S = {}^1/_2$ region ($g = 2.01$,1.94, 1.92, see Figure 4B) is much closer to that of mammalian-type 2Fe Fds (typically $g = 2.02$, 1.94, 1.94 (*30*)) than plant-type 2Fe Fds (typically $g = 2.05$, 1.96, 1.88 (*31*)). By analogy with mammalian-type Fds, the RR and EPR data taken together add strong support to the view that the cluster in the C14A/Q21C/C60A/S61A protein is ligated by four cysteinyl residues.

An unexpected complication is that both EPR and VTMCD studies of the C14A/Q21C/C60A/S61A variant indicate spin state heterogeneity in the reduced samples. As the temperature is increased to 40 K, a sharp isotropic resonance centered at $g = 5.16$ is observed in the low field region of the EPR spectrum (data not shown). Under the assumption that zero-field splitting is much larger than the Zeeman splitting, this resonance can only be interpreted as arising from the $M_s = {}^3/_2$ doublet of a $S = {}^7/_2$ ground state with $E/D \sim 0.12$ and $D < 0$. Evidence for a high spin species is also apparent by the appearance and anomalous temperature dependence of a band centered at 770 nm in the VTMCD spectrum, see Figure 5B. By analogy with our studies of VTMCD properties of valence-delocalized $S = {}^9/_2$ $[2Fe-2S]^+$ clusters in the C56S and C60S variants of *Cp* 2Fe Fd (*6*, *23*), a high spin $[2Fe-2S]^+$ cluster is likely to have intense positive bands in the 400−500 nm region. Hence detailed comparison of the VTMCD spectrum of the C14A/Q21C/C60A/S61A variant with those of other $S = {}^1/_2$ $[2Fe-2S]^+$ clusters in 2Fe Fds is not meaningful at this time. Work is in progress to understand the origin of the spin state heterogeneity and to characterize the electronic, magnetic, vibrational, and valence delocalization properties of both the $S = {}^1/_2$ and ${}^7/_2$ forms of this mutated form.

The redox potential of the C14A/Q21C/C60A/S61A variant (−406 mV, Table 2) is ∼120 mV more negative than those of the WT and mammalian-type Fds, but near those measured for plant-type Fds (*32*). In light of the spectroscopic results discussed above, we conclude that the redox potential is determined by the overall cluster environment, rather than by the specific arrangement of coordinating cysteine residues. Further support for this conclusion comes from the observation that redox potential shifts of similar magnitude have previously been observed upon cysteine swapping and deletions in the flexible loop encompassing residues 17−32 (*7*), that is, structural modifications apparently unrelated to those carried out here. The redox potential of the C14A/Q21C/C60A/S61A variant is the lowest so far for any mutated form of *Cp* 2Fe Fd having four cysteine ligands (see below) and expands the redox potential range encompassed by this set of variants to 126 mV.

The spectroscopic properties of the C14A/Q21C/C60A/S61A variant shown above are suggestive of an all-cysteine ligated [2Fe-2S] cluster. This is in addition supported by a

number of molecular variants (Tables 1 and 2). Concerning cysteine 56, the absence of chromophore in the C56A variant strongly suggests that this ligand is indispensable, and that ligand swapping (for instance with cysteine 14) is unlikely to occur at this site. Furthermore, the C14A/Q21C/C56A protein is unable to stabilize any chromophore (Table 2), which shows that cysteine 21 cannot compensate for the absence of cysteine 56. As to cysteine 11, the low stability and production yield of the C11S variant (*5*) and the absence of chromophore in the C11A variant (Table 2) suggest that ligand exchange on this site is very unlikely in the WT context. Furthermore, incorporation of the C11A mutation into the C14A/Q21C/C60A/S61A background (Tables 1 and 2) produced a variant unable to stabilize a chromophore. It is therefore most probable that cysteines 11 and 56 are ligands of the cluster in the C14A/Q21C/C60A/S61A variant at the same sites as in WT Fd. The increased stability of the chromophore (Table 2) and the spectral changes (Figure 6) resulting from the introduction of cysteine 21 provide strong evidence that this residue is a cluster ligand in the C14A/Q21C/C60A/S61A protein. The fourth ligand must be cysteine 24, as the C14A/Q21C/C24A/C60A/S61A variant, which was obtained by incorporating the C24A mutation into the C14A/Q21C/C60A/S61A mutated plasmid, was unable to assemble a chromophore. Thus, the cluster ligands are cysteines 11, 21, 24, and 56 in the C14A/Q21C/C60A/S61A variant. The simplest picture would consist of cysteines 11, 24, and 56 as ligands at the same sites as in the WT protein, and cysteine 21 as substitute for cysteine 60. However, in view of the flexibility of the polypeptide chain near cysteines 24 (*5*, *7*) and 60 (this work), one may consider an alternative situation in which cysteines 21 and 24 would have swapped positions. Further structural data are wanted to solve this issue.

CONCLUSIONS

The *Cp* 2Fe Fd had previously been shown to contain a [2Fe-2S] cluster coordinated by cysteine residues 11, 56, and 60 and by a fourth cysteine, residue 24 in the WT protein, located on a flexible and deletable loop encompassing the 19−30 region of the sequence (*5*, *7*). A number of new mutated forms have been described here, and the data now available show that in the full-length protein, and with appropriate mutations, the fourth cysteine ligand may be placed in any one of positions 14, 16, 21, 24, and 26. Such extensive ligand swapping is unprecedented in Fe−S proteins. These variants alone cover a redox potential range of nearly 80 mV (ref *7*; Table 2). Altogether, the *Cp* 2Fe Fd variants having an all-cysteine ligated [2Fe-2S] cluster span a redox potential range of 126 mV (from −406 to −280 mV) (ref *7*; this work).

The most significant and unexpected finding reported here is the observation that ligand swapping may occur at the cysteine 60 ligand site as well. When the latter residue is mutated into alanine, the all-cysteinyl coordination of the [2Fe-2S] cluster can be restored by the introduction of a cysteine residue in position 21. In this case, as shown by spectroscopic data and by a number of molecular variants, the ligands of the [2Fe-2S] cluster are cysteines 11, 21, 24, and 56. Quite remarkably, this pattern of cysteine distribution is reminiscent of the one found in plant and in mammalian Fd (*32*). This result was unexpected, since, according to its primary structure and cysteine ligand pattern (*1*), *Cp* 2Fe Fd appeared to be totally unrelated to plant-type or mammalian-type Fds. The data suggest either that *Cp* 2Fe Fd is flexible enough to assume, upon limited sequence alterations, a similar fold around its [2Fe-2S] site as mammalian-type Fd or that there are more structural similarities between the two types of proteins than previously estimated. However, in light of the CD results which indicate very different protein folding in the vicinity of the cluster compared to plant- or mammalian-type Fds, the similarity of the cysteine ligand pattern may well be mere coincidence. Answers to these questions obviously call for structural data on *Cp* 2Fe Fd. The latter protein had previously been shown to share similarities in sequence and chromophore structure with the 25 kDa subunit of mitochondrial and bacterial proton-translocating NADH/ubiquinone oxidoreductase, and these similarities have been increased by appropriate mutations (*7*). *Cp* 2Fe Fd thus appears to be an exceptionnally versatile structure having the potential to mimick a wide range of [2Fe-2S] proteins.

The availability of two ligand sites, cysteines 24 and 60, amenable to ligand swapping has been an incentive for the preparation of noncysteine ligated [2Fe-2S] clusters. Several residues with iron-coordinating potential, namely aspartate, asparagine, histidine, or methionine, have been introduced in positions where cysteine ligation had been proven to be possible, and where the flexibility of the polypeptide chain, as inferred from cysteine ligand swapping, might allow structural readjustments required by the steric properties of the newly introduced residues. However, none of these mutations, in positions 16, 21, 24, or 60, resulted in any modifications of the UV−vis absorption spectra, thus indicating that cysteine alone, among the residues tested, can be a ligand of the Fe−S cluster in these positions. Other mutated forms prepared previously (*5*) and in this work (Tables 1 and 2) have shown that neither serine residues introduced in position 14 or 24 nor the native serines in position 13, 26, 29, or 61 are ligands of the Fe−S cluster in any of the tested molecular forms of the Fd. Thus, among the many variants obtained so far with this protein, only the C56S, C60S, and probably C11S ones have been shown to contain a [2Fe-2S] cluster with a noncysteinyl ligand. This low rate of success most likely results from the strong preference of iron−sulfur clusters for thiolate ligation (*9*, *10*) and reflects the relatively rare occurrence of noncysteinyl ligation in native Fe−S proteins (*24*).

Previous studies had shown that cysteines 56 and 60 are the ligands of the reducible iron (*4*−*6*) and that the cysteine 24 ligand site is relatively labile (*5*, *7*). The data reported here show that the cysteine 60 ligand site can also undergo ligand swapping, whereas cysteines 11 and 56 appear to be mandatory. This would be consistent with an active site located near the surface of the protein, with cysteines 11 and 56 on the internal side, and therefore having limited freedom for substitution or swapping, and with cysteines 24 and 60 on the external side, and thus more likely to undergo various kinds of exchange reactions (Figure 8). Interestingly, despite the presence of two relatively labile ligand sites, the vast majority of molecular variants of *Cp* 2Fe Fd assembles an Fe−S chromophore and in all known cases a [2Fe-2S] cluster. This suggests that a significant amount of stabilizing energy is transferred to the cluster by the protein through

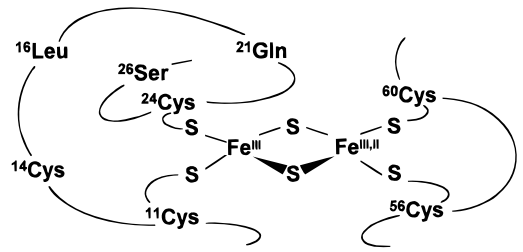

FIGURE 8: Tentative scheme of the [2Fe-2S] active site environment of *Cp* 2Fe Fd. Although the actual structure of the protein is unknown, this scheme is aimed at summarizing the information collected from site-directed mutagenesis. Cysteines 56 and 60 are indicated as ligands of the reducible iron. Those residues that may become ligands of the cluster upon mutation into cysteine are shown. Glutamine 21, when mutated into cysteine, may be a ligand of either iron atom, depending on the molecular variant considered. The lower part of the iron−sulfur cluster is meant to be oriented toward the hydrophobic core of the protein, whereas the upper part is most likely solvent-exposed.

the more rigid part of the ligand framework, namely cysteines 11 and 56. The cluster is thereby allowed, under appropriate conditions, to drive ligand exchange and protein rearrangements on its more accessible side. The bearings of these unique properties on the putative function (*33*) of *Cp* 2Fe Fd are currently being investigated.

REFERENCES

1. Meyer, J., Bruschi, M. H., Bonicel, J. J., and Bovier-Lapierre, G. E. (1986) *Biochemistry 25*, 6054−6061.
2. Meyer, J., Moulis, J.-M., and Lutz, M. (1986) *Biochim. Biophys. Acta 873*, 108−118.
3. Meyer, J., Moulis, J.-M., Gaillard, J., and Lutz, M. (1992) *Adv. Inorg. Chem. 38*, 73−115.
4. Fujinaga, J., Gaillard, J., and Meyer, J. (1993) *Biochem. Biophys. Res. Commun. 194*, 104−111.
5. Meyer, J., Fujinaga, J., Gaillard, J., and Lutz, M. (1994) *Biochemistry 33*, 13642−13650.
6. Crouse, B. R., Meyer, J., and Johnson, M. K. (1995) *J. Am. Chem. Soc. 117*, 9612−9213.
7. Golinelli, M.-P., Akin, L. A., Crouse, B. R., Johnson, M. K., and Meyer, J. (1996) *Biochemistry 35*, 8995−9002.
8. Achim, C., Golinelli, M.-P., Bominaar, E. L., Meyer, J., and Münck, E. (1996) *J. Am. Chem. Soc. 118*, 8168−8169.
9. Zhou, C., and Holm, R. H. (1997) *Inorg. Chem. 36*, 4066−4077.
10. Beinert, H., Holm, R. H., and Münck, E. (1997) *Science 277*, 653−659.
11. Machray, G. C., Burch, L., Hedley, P. E., Davies, H. V., and Waugh, R. (1994) *FEBS Lett. 354*, 123−127.
12. Ausubel, F. M., Brent, R., Kingston, R. E., Moore, D. D., Seidman, J. G., Smith, J. A., and Struhl, K. (1987−1998) *Current Protocols in Molecular Biology*, Wiley-Interscience, New York.
13. Fujinaga, J., and Meyer, J. (1993) *Biochem. Biophys. Res. Commun. 192*, 1115−1122.
14. Kammann, M., Laufs, J., Schell, J., and Gronenborn, B. (1989) *Nucleic Acids Res. 17*, 5404.
15. Higuchi, R., Krummel, B., and Saiki, R. K. (1988) *Nucleic Acids Res. 16*, 7351−7365.
16. Tabor, S. (1990) Expression using the T7 RNA Polymerase/Promoter System, in *Current Protocols in Molecular Biology* (Ausubel, F. M., Brent, R., Kingston, R. E., Moore, D. D., Seidman, J. G., Smith, J. A., and Struhl, K., Eds.) pp 16.2.1−16.2.11, Wiley-Interscience, New York.
17. Quinkal, I., Davasse, V., Gaillard, J., and Moulis, J.-M. (1994) *Protein Eng. 7*, 681−687.
18. Han, S., Czernuszewicz, R. S., Kimura, T., Adams, M. W. W., and Spiro, T. G. (1989) *J. Am. Chem. Soc. 111*, 3505−3511.
19. Fu, W., Drozdzewski, P. M., Davies, M. D., Sligar, S. G., and Johnson, M. K. (1992) *J. Biol. Chem. 267*, 15502−15510.
20. Bertrand, P., Guigliarelli, B., Gayda, J.-P., Beardwood, P., and Gibson, J. F. (1985) *Biochim. Biophys. Acta 831*, 261−266.
21. Werth, M. T., Cecchini, G., Manodori, A., Ackrell, B. A. C., Schröder, I., Gunsalus, R. P., and Johnson, M. K. (1990) *Proc. Natl. Acad. Sci. U.S.A. 87*, 8965−8969.
22. Shen, B., Jollie, D. R., Diller, T. C., Stout, C. D., Stephens, P. J., and Burgess, B. K. (1995) *Proc. Natl. Acad. Sci. U.S.A. 92*, 10064−10068.
23. Johnson, M. K., Duin, E. C., Crouse, B. R., Golinelli, M.-P., and Meyer, J. (1998) in *Spectroscopic Methods in Bioinorganic Chemistry* (Solomon, E. I., and Hodgson, K. O., Eds.) ACS Symposium Series, Washington D. C. (in press).
24. Moulis, J.-M., Davasse, V., Golinelli, M.-P., Meyer, J., and Quinkal, I. (1996) *J. Biol. Inorg. Chem. 1*, 2−14.
25. Shergill, J. K., Golinelli, M.-P., Cammack, R., and Meyer, J. (1996) *Biochemistry 35*, 12842−12848.
26. Matsubara, H., and Saeki, K. (1992) *Adv. Inorg. Chem. 38*, 223−280.
27. Meyer, J., Moulis, J.-M., and Lutz, M. (1984) *Biochem. Biophys. Res. Commun. 119*, 828−835.
28. Stephens, P. J., Thomson, A. J., Dunn, J. B. R., Keiderling, T. A., Rawlings, J., Rao, K. K., and Hall, D. O. (1978) *Biochemistry 17*, 4770−4778.
29. Ta, D. T., and Vickery, L. E. (1992) *J. Biol. Chem. 267*, 11120−11125.
30. Xia, B., Cheng, H., Bandarian, V., Reed, G. H., and Markley, J. L. (1996) *Biochemistry 35*, 9488−9495.
31. Cheng, H., Xia, B., Reed, G. H., and Markley, J. L. (1994) *Biochemistry 33*, 3155−3164.
32. Johnson, M. K. (1994) in *Encyclopedia of Inorganic Chemistry* (King, R. B., Ed.) Vol. 4, pp 1896−1915, Wiley, U.K.
33. Golinelli, M.-P., Gagnon, J., and Meyer, J. (1997) *Biochemistry 36*, 11797−11803.
34. Takahashi, Y., Hase, T., Wada, K., and Matsubara, H. (1983) *Plant Cell Physiol. 24*, 189−198.

BI9806394